Proceedings of the Combustion Institute 40 (2024) 105291

Contents lists available at ScienceDirect

Proceedings of the Combustion Institute

journal homepage: www.elsevier.com/locate/proci

A numerically-stable method for enforcing numerical conservation in transported probability density function models: Application to MMC-IEM with one reference variable

Andrew P. Wandel

School of Engineering, University of Southern Queensland, Toowoomba, Qld, 4350, Australia

ARTICLE INFO

Keywords:
Transported probability density function models
Multiple mapping conditioning
Interaction by exchange with the mean
Conservative numerical methods

ABSTRACT

Turbulent combustion closure models – for Transported Probability Density Function (TPDF) models – where more than one other stochastic particle influences the mixing process for any given particle may not be mathematically conservative. A technique is proposed here which makes the mixing process conservative within numerical precision by correcting the matrix governing the contribution each particle makes to each particle's new value. In each iteration, the matrix is normalised to become conservative, then renormalised to become well-mixed so that it complies with numerical stability requirements. The technique inherently converges until the error in conservation is lower than the desired tolerance. This technique is tested on the Multiple Mapping Conditioning (MMC) model using the Interaction-by-Exchange-with-the-Mean (IEM) model for the turbulent micro-mixing closure (MMC-IEM) for the approach where the two closest particles in reference space are used to compute the conditional mean towards which a particle relaxes. For a single reference variable, these two particles are the immediate neighbour in either direction in reference space. While this method is implicitly conservative if all particles have identical weights, it is inherently unconservative otherwise. This is a challenge for applying this method to standard inhomogeneous combustion codes, where varying particle weights is used to manage computational load and accuracy by removing stochastic particles if there are too many in a region and creating stochastic particles if there are insufficient. The technique is tested using an inhomogeneous lifted-flame open flow, with the introduction of numerical conservation having an insignificant impact on the mean results, so the essence of MMC-IEM is preserved. The conservation error in the scalars is 3 orders of magnitude lower than the specified tolerance for the matrix. However, because the chemical kinetics scheme only used 48 species – of which, 28 were steady-state – it is expected that the application of this technique to practical cases with more species and at higher pressures will have a more significant impact.

1. Introduction

As the world seeks to transition away from fossil fuels, in a number of sectors combustion remains advantageous compared to electrification. In the aviation industry for instance [1], batteries have significantly lower energy density than fuels; fuel consumption reduces the weight of aircraft during flight, thereby increasing range; and the efficiency of aircraft at cruising altitude means that their CO_2 emissions are lower than conventional electricity generation. The major challenges facing combustion of alternative fuels is to operate as lean as possible for maximum reduction in pollution, but still maintain a stable flame [2,3]. To be able to design such systems requires accurate modelling of extinction-reignition phenomena [4].

The Multiple Mapping Conditioning (MMC) model [5,6] provides a framework that has been successfully used to model extinction-reignition phenomena. Key to its design is the reference variable which is used for conditioning: this reference space is mapped to the main scalars and permits the model to govern the locality of mixing.

Section 2 derives the criteria that are to be met for a mixing model to perform correctly, then Section 3 proves that MMC-IEM fails to comply with all of these criteria. Section 4 introduces a technique that can be used to make any Transported Probability Density Function model compliant within numerical precision, followed by a demonstration of this technique using MMC-IEM in Section 5 and conclusions in Section 6.

E-mail address: andrew.wandel@unisq.edu.au.

https://doi.org/10.1016/j.proci.2024.105291
Received 4 December 2023; Accepted 22 May 2024
Available online 21 November 2024

2. Numerical properties of mixing processes

Let ϕ_i^k be the value of any variable ϕ for particle i at time instant k. The interaction process is defined to have all particles explicitly influence the value of each particle to determine the new value:

$$\phi_i^{k+1} = \sum_j L_{ij}\phi_j^k\,, \tag{1}$$

where L_{ij} represents the elements of the interaction matrix $\mathbf{L}$. The matrix for the rate of interaction, $\mathbf{M}$, can also be defined [7]:

$$W_i d\phi_i = -\sum_j M_{ij}\phi_j^k dt\,, \tag{2}$$

where W_i is the weight of particle i (its mass or probability) and the Einsteinian summation convention is not used. Assuming simple upwinding to discretise the change in ϕ, substitution of Eq. (1) into Eq. (2) yields (δ_{ij} is the Kronecker δ-function):

$$L_{ij} \equiv \delta_{ij} - M_{ij}dt/W_i\,. \tag{3}$$

If a scheme is conservative, then the entire amount of each particle is distributed precisely to the particle field – nothing from an individual particle is lost or gained. For Eq. (1) to be conservative – which means that the mean value of the field ϕ is unchanged by the operation Eq. (1) – the sum of the elements in each column must be [7]:

$$\forall_j \sum_i M_{ij} = 0\,, \quad \forall_j \sum_i W_i[\delta_{ij} - L_{ij}] = 0\,. \tag{4}$$

After some basic algebra, the conditions to satisfy conservation, Eq. (4), are:

$$\forall_j \sum_i M_{ij} = 0\,, \quad \forall_j \frac{1}{W_j}\sum_i W_i L_{ij} = 1\,. \tag{5}$$

If $\forall_i W_i = W$, then Eq. (5) becomes $\forall_j \sum_i L_{ij} = 1$. A consequence of Eq. (5) is that the solution of Eq. (1) is bounded [7]: $\min(\phi_i^k) \le \phi_i^{k+1} \le \max(\phi_i^k)$. Ensuring that the mixing process is conservative is especially important for spray processes, because the gaseous mixture fraction is no longer conservative due to the source created by the droplet evaporation. This change in the behaviour of the mixture fraction poses challenges for the modelling of these systems, especially because any change in conservation cannot be attributed to numerical errors [8].

If a scheme is "well-mixed", then each particle receives the same total mass fraction that it distributed to the particle field. For Eq. (1) to be numerically stable, it is necessary for $\mathbf{L}$ to be well-mixed; mathematically, the sum of the elements in each row must be:

$$\forall_i \sum_j M_{ij} = 0\,, \quad \forall_i \sum_j L_{ij} = 1\,. \tag{6}$$

A consequence of Eq. (6) is that a uniform solution is preserved by Eq. (1): if $\forall_i \phi_i^k = \phi$, then $\forall_i \phi_i^{k+1} = \phi$. In other words, the enforcement of Eq. (6) guarantees numerical stability because the solution of Eq. (1) does not introduce numerical fluctuations in the value of ϕ_i^{k+1} – which would likely be divergent.

There are a number of other properties that the formula for M_{ij} should obey for physical modelling [7]. The physical properties that are not directly addressed in this work are localness of mixing and relaxation to a Gaussian distribution in homogeneous turbulence. The remaining mathematical property that M_{ij} must obey for turbulent mixing [7] ensures that the dissipation of the covariance of multiple scalars ϕ and φ complies with the covariance transport equation (which also ensures variance decay [7]). To achieve compliance, $\mathbf{M}_s \equiv \frac{1}{2}[\mathbf{M} + \mathbf{M}^{\mathrm{T}}]$ (the symmetric part of $\mathbf{M}$) must be a positive semi-definite matrix; to satisfy this requirement, $\mathbf{M}_s$ must be symmetric and all its eigenvalues must be non-negative.

Depending on the weighting kernel used to define the elements M_{ij}, $\mathbf{M}$ can be sparse, and this is a desirable feature when particle j is distant from i because it enforces localness.

3. Compliance of IEM with the numerical conditions

The Interaction-by-Exchange-with-the-Mean (IEM) model [9,10], which has the variant Interaction-by-Exchange-with-the-Conditional-Mean (IECM) [11–13], has the following formula for the mixing substep:

$$d\phi_i = -\frac{\phi_i - \langle\phi\rangle}{\tau}dt\,, \tag{7}$$

where $\langle\phi\rangle$ is the (local) mean of ϕ and τ is an appropriately-defined mixing timescale.

It is common to compute the mean discretely:

$$\langle\phi\rangle = \frac{\sum_j W_j\phi_j}{\sum_j W_j} = \sum_j \frac{W_j\phi_j}{\sum_l W_l}\,, \tag{8}$$

therefore Eq. (7) becomes

$$d\phi_i = -\frac{dt}{\tau}\left(\phi_i - \sum_j \frac{W_j\phi_j}{\sum_l W_l}\right). \tag{9}$$

Substituting into Eq. (2) yields for discrete IEM:

$$M_{ij} \equiv \frac{W_i}{\tau}\left(\delta_{ij} - \frac{W_j}{\sum_l W_l}\right). \tag{10}$$

Any particle not involved in computing $\langle\phi\rangle$ (because it is in a different region of space) can be assigned $W_j = W_l = 0$ for the purposes of computing Eq. (10).

The proof that Eq. (10) satisfies Eq. (6), and is therefore well-mixed, is:

$$\begin{aligned}\sum_j M_{ij} &= \frac{W_i}{\tau}\left(\sum_j \delta_{ij} - \sum_j \frac{W_j}{\sum_l W_l}\right)\\ &= \frac{W_i}{\tau}\left(1 - \frac{\sum_j W_j}{\sum_l W_l}\right) = \frac{W_i}{\tau}(1-1) = 0\,.\end{aligned}$$

The proof that discrete IEM is conservative — because Eq. (10) satisfies Eq. (5) is:

$$\begin{aligned}\sum_i M_{ij} &= \sum_i \frac{W_i}{\tau}\delta_{ij} - \sum_i \frac{W_i}{\tau}\frac{W_j}{\sum_l W_l}\\ &= \frac{W_j}{\tau} - \frac{\sum_i W_i}{\tau}\frac{W_j}{\sum_l W_l} = \frac{W_j}{\tau} - \frac{W_j}{\tau} = 0\,.\end{aligned}$$

However, in order for Eq. (5) to be satisfied for any valid specification of W_j, all particles j must have the same value of $\langle\phi\rangle$ as particle i; in other words, the calculation of $\langle\phi\rangle$ must be segregated – the particles must be grouped so that they exclusively contribute to the computation of $\langle\phi\rangle$ for that group; in other words, $\mathbf{M}$ must be a block diagonal matrix.

3.1. Pairwise models

For pairwise models, where each particle's value of ϕ only changes due to the values of ϕ for the two particles in the pair, $\mathbf{M}$ can be defined for each pair of particles to be:

$$\mathbf{M} = m^{\{ij\}}\begin{bmatrix} 1 & -1 \\ -1 & 1 \end{bmatrix}, \tag{11}$$

where $m^{\{ij\}}$ is some scalar coefficient for each particle pair that is defined by the specific model. Every pairwise model satisfies both the well-mixed and conservation criteria, Eqs. (5) and (6) respectively, irrespective of the method used to simulate the mixing, i.e. irrespective of the formula used for $m^{\{ij\}}$.

The Modified Curl's model [14,15] is one of the most common pairwise models, where $m^{\{ij\}}$ is chosen independently for each pairing. The other most commonly-used pairwise model is EMST [7], where each particle may be paired with multiple other particles; while Eq. (11) is applied for each pairing (hence the method is inherently both conservative and well-mixed), $m^{\{ij\}}$ is dependent on the values determined for other pairs (which is why EMST is not linear).

3.2. MMC

Multiple Mapping Conditioning (MMC) [5] introduces a conditioning variable ξ which is used to enforce locality on the transport of ϕ. Modern applications of MMC exclusively use a stochastic approach, with numerous closures for the mixing process devised described below. Fundamental to all methods is the concept of a "minor" mixing timescale τ_c, which governs the rate of decay of ϕ to $\langle\phi|\xi\rangle$. This obeys $\tau_c < \tau$ if there is a significant correlation between ϕ and ξ, with τ_c/τ monotonically decreasing with increasing correlation [16,17] between ϕ and ξ.

One approach to closing the mixing process is called "MMC-Curl" [16–21], where the Modified Curl's model [14,15] is used to compute the amount by which the particles share their values. Particles are paired based on closeness in reference space and only some particles mix each timestep.

Most MMC implementations use an IEM closure:

$$\phi_i^{k+1} = \phi_i^k - \frac{\phi_i^k - \langle\phi|\xi_i\rangle}{\tau_c}\Delta t\,, \tag{12}$$

with the principal difference between those implementations the method used to compute $\langle\phi|\xi_i\rangle$. Note that the minor timescale is necessary in Eq. (12) – but is not necessary in IECM [11–13] – because the conditioning variable ξ is normally associated with ϕ directly or via another scalar. This correlation by definition between ϕ and ξ means that $|\phi_i^k - \langle\phi|\xi_i\rangle|$ is normally significantly smaller than $|\phi_i^k - \langle\phi\rangle|$. However, in IECM $|\phi_i^k - \langle\phi|\mathbf{U}_i\rangle|$ is approximately the same as $|\phi_i^k - \langle\phi\rangle|$ because there is fundamentally no requirement for ϕ and $\mathbf{U}$ to be correlated, although they almost certainly have at least some correlation in practice.

The most widely-used method in MMC, used in MMC-LES [22,23] and some RANS [24–26], defines $\langle\phi|\xi_i\rangle$ by pairing particle i with some particle j that is nearby in ξ-space and computing $\langle\phi|\xi_i\rangle$ using the weighted mean of ϕ_i and ϕ_j. Because this can also be formulated as a Modified Curl's [14,15] method, this method is called "MMC-Curl-IEM" here. By being a pairwise method, it is implicitly conservative [7].

The method called "MMC-IEM" [27–30] solves Eq. (12) by computing $\langle\phi|\xi_i\rangle$ as the weighted mean of the particles either side of particle i:

$$\langle\phi|\xi_i\rangle = \frac{W_{i-1}\phi_{i-1}^k + W_{i+1}\phi_{i+1}^k}{W_{i-1}+W_{i+1}}\,. \tag{13}$$

Eq. (12) becomes:

$$\begin{aligned} d\phi &= -\frac{dt}{\tau_c}\left(\phi_i^k - \frac{W_{i-1}\phi_{i-1}^k + W_{i+1}\phi_{i+1}^k}{W_{i-1}+W_{i+1}}\right) \\ M_{ij} &= \frac{W_i}{\tau_c}\left\{\delta_{ij} - \left[\frac{W_{j+1}\delta_{i(j+1)} + W_{j-1}\delta_{i(j-1)}}{W_{j+1}+W_{j-1}}\right]\right\} \end{aligned} \tag{14}$$

making $\mathbf{M}$ a tri-diagonal matrix. The particles at either end require a boundary condition: the particle acts as a ghost particle for the absent particle that would be outside the range of existing particles [30]. For the first few particles, the interaction matrix is:

$$L_{\{1-3\}\{1-3\}} = \begin{bmatrix} 1-\frac{dt}{\tau_c}(1-\frac{W_1}{W_1+W_2}) & \frac{dt}{\tau_c}\frac{W_2}{W_1+W_2} & 0 \\ \frac{dt}{\tau_c}\frac{W_1}{W_1+W_3} & 1-\frac{dt}{\tau_c} & \frac{dt}{\tau_c}\frac{W_3}{W_1+W_3} \\ 0 & \frac{dt}{\tau_c}\frac{W_2}{W_2+W_4} & 1-\frac{dt}{\tau_c} \end{bmatrix} \tag{15}$$

It is straightforward to prove that this scheme satisfies Eq. (6). It is, however, only conservative if all the weights are identical (refer to Appendix for the proof). Since inhomogeneous codes rely on the weights being different for each particle, this poses challenges for this method. To rectify this problem, it is inadvisable to attempt to correct the values so that the mean is preserved following the (unconservative) mixing process. This is because the cell mean is computed using every particle, so M_{ij} has no non-zero elements, and the method almost certainly violates the well-mixed criterion. A robust technique to make this scheme conservative is presented in Section 4.

3.3. PSP model

The Parameterised Scalar Profiles (PSP) model [31] is very similar to the MMC-IEM model in that Eq. (12) is solved with a conditional mean computed using Eq. (13) (albeit PSP is only formulated with uniform weights W): two particles are chosen, with one of those particles' value of ϕ being no greater than ϕ_i and the other being no smaller than ϕ_i. However, the principal difference between PSP and MMC-IEM is that in PSP the two particles chosen to compute Eq. (13) are randomly selected from those particles in the computational cell – instead of those immediately closest – and the selection persists until either the difference between the chosen particle's ϕ and ϕ_i changes sign (i.e. they change order), or a certain time has elapsed (randomly chosen, based on the turbulent mixing frequency). A further variation is that in PSP τ_c for each particle is solved using a stochastic differential equation for the frequency $1/\tau_c$.

It can therefore be concluded that this primary definition of PSP is well-mixed. However, it is inherently not conservative – even if the particles have the same weight – because $\mathbf{M}$ is not a tri-diagonal matrix. This problem was recognised in the original formulation of PSP [31], with a correction applied by using a weighted sum of the changes $d\phi_i \equiv \phi_i^{k+1} - \phi_i^k$ computed by Eq. (12). However, as noted earlier, while this approach causes the method to become conservative (ergo bounded), it is no longer well mixed. It can therefore be concluded that PSP is another candidate model for the approach described in the next section.

4. Numerical technique to enforce conservation

The scheme described here [32] enables any interaction matrix $\mathbf{L}$ to become conservative to the desired numerical precision. Let the errors for conservation and well-mixedness, $\epsilon_{c,j}$ and $\epsilon_{w,i}$ respectively, be defined so that:

$$\frac{1}{W_j}\sum_i W_i L_{ij} = (1+\epsilon_{c,j})\times 1 \tag{16}$$

$$\sum_j L_{ij} = (1+\epsilon_{w,i})\times 1\,. \tag{17}$$

If $\forall_j \epsilon_{c,j} = 0$, then the matrix $\mathbf{L}$ is conservative by virtue of Eq. (5); if $\forall_i \epsilon_{w,i} = 0$, then the matrix $\mathbf{L}$ is well-mixed by virtue of Eq. (6). Since the errors can be attributed to any element in the entire row/column of $\mathbf{L}$, it is possible to normalise $\mathbf{L}$ using these errors to ensure compliance.

The procedure to make $\mathbf{L}$ conservative is, for iteration m:

1. Compute the error in conservation for the well-mixed matrix L_{ij}^m using Eq. (16).
2. Make the well-mixed matrix L_{ij}^m conservative:
$$\forall_{i,j}\,\hat{L}_{ij}^m = L_{ij}^m \div \left(1+\epsilon_{c,j}^m\right)\,. \tag{18}$$
3. Compute the error in well-mixedness for the conservative matrix $\hat{L}_{ij}^m$ using Eq. (17).
4. Make the conservative matrix $\hat{L}_{ij}^m$ well-mixed:
$$\forall_{i,j}\,L_{ij}^{m+1} = \hat{L}_{ij}^m \div \left(1+\epsilon_{w,i}^m\right)\,. \tag{19}$$

This should be repeated until $\max(|\epsilon_{c,j}^m|)$ is lower than the desired error tolerance ϵ. Tests for different distributions of W_i using a tri-diagonal matrix found that this scheme always converges.

5. Validation of the technique

The binomial Langevin-MMC (BLM-MMC) framework [20,21] was used, with the binomial Langevin mixture fraction [33] used to define the reference variable:

$$d\eta_i = \frac{G_\eta}{2\tau}\left(\eta_i - \langle\eta\rangle\right)dt + \left(B_\eta\langle\varepsilon_\eta\rangle\right)^{1/2} dw_{\text{bin}}\,. \tag{20}$$

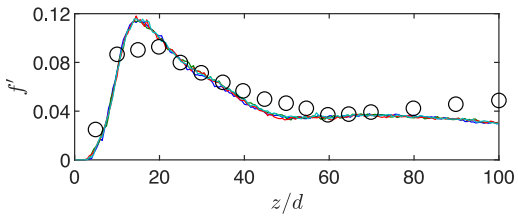

Fig. 1. Ensemble mean of centreline Favre-averaged mixture fraction rms for $\tau_c/\tau = 1/8$. Unconservative ($\epsilon = 10^{-2}$), —; $\epsilon = 10^{-3}$, —; 10^{-4}, —; 10^{-5}, —. Experiment [35], ∘.

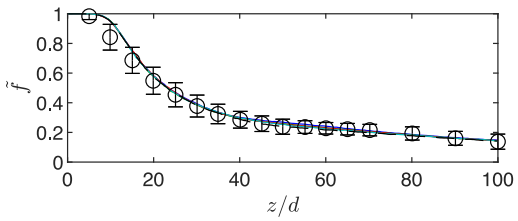

Fig. 2. Ensemble mean of centreline Favre-averaged mixture fraction for $\epsilon = 10^{-5}$. $\tau_c/\tau = 1/8$, —; 1/4, —; 1/3, —; 1/2, —. BLM-MMC-Curl [21], – –. Experiment [35], ∘.

Table 1
95% confidence intervals (CI) for the conservation error in **L** and consequential absolute error in mean mixture fraction for each instance of Eq. (1). The final column is the mean additional computational time required to complete the simulations relative to $\epsilon = 10^{-2}$. Results are for different error tolerances ϵ for $\tau_c/\tau = 1/8$.

ϵ	**L** error		$\langle Z \rangle$ error		Δt_{CPU}
	Lower CI	Upper CI	Lower CI	Upper CI	
10^{-2}	0.5704×10^{-2}	0.5727×10^{-2}	0.3098×10^{-5}	0.3193×10^{-5}	0%
10^{-3}	0.8631×10^{-3}	0.8644×10^{-3}	0.3835×10^{-6}	0.3951×10^{-6}	0.24%
10^{-4}	0.9739×10^{-4}	0.9749×10^{-4}	0.4802×10^{-7}	0.4936×10^{-7}	1.46%
10^{-5}	0.9952×10^{-5}	0.9958×10^{-5}	0.6518×10^{-8}	0.6703×10^{-8}	3.34%

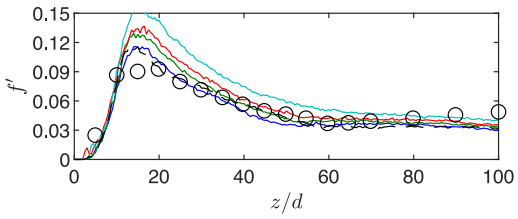

Fig. 3. Ensemble mean of centreline Favre-averaged mixture fraction rms. As per Fig. 2.

Here G_η is the drift coefficient, B_η the diffusion coefficient, dw_{bin} is a binomial Wiener process [34] and the mean scalar dissipation is modelled as $\langle \varepsilon_\eta \rangle \equiv \langle \eta'^2 \rangle / \tau$, with the scalar timescale proportional to the turbulent timescale τ_u using the standard form $\tau = \tau_u / C_\phi$ ($C_\phi = 2.0$). The MMC scalars evolve according to:

$$dZ^{*p} = S dt \tag{21}$$

$$dY_I^{*p} = (S + \mathcal{W}_I) dt\,, \tag{22}$$

where Z is the MMC mixture fraction, Y_I are the reactive scalars, $\mathcal{W}_I$ is the chemical source term, and S is modelled using Eq. (2).

The test case was an experiment of a methane-air jet with vitiated coflow [35], which has been extensively used as a test case for turbulent combustion models [36–41]. The jet had 33% v.v. CH_4 at room temperature, while the coflow was lean H_2 (equivalence ratio of 0.4) that was burned (to 1350 K) prior to entering the experimental zone. The jet's pipe diameter was $d = 4.57$ mm and flowed at 100 m/s, while the coflow speed was 5.4 m/s. Because the ignition of the primary jet relies on sufficient mixing with the co-flow, a lifted flame is produced, while the jet Reynolds number of 28,000 causes significant extinction-reignition to occur, which, by design, is challenging for turbulent combustion models to predict.

The technique was implemented into the parabolic PIPER code [42], with a reduced chemical mechanism for methane that uses 48 species, 28 of which are steady-state, and 300 reactions [43]. The turbulence is modelled using a Reynolds stress model [44] with the triple moments and pressure transport terms closed using the generalised gradient diffusion formulation [45], while the standard turbulent kinetic energy dissipation rate model [46] is used with $C_{\varepsilon 2}$ changed from 1.92 to 1.8 to better predict the spreading rate.

It has previously been proven for homogeneous combustion that the effect of renormalisation causes minimal deviations in the results compared to the implicitly-conservative scheme with uniform particle weight [47]. That work also found that the resultant error in mixture fraction conservation was approximately 5 orders of magnitude smaller than the error tolerance ϵ specified to be the maximum allowable value of $\epsilon_{c,j}$.

The compliance of the technique with the covariance transport equation was checked for $\mathbf{M}_s$. Cholesky factorisation [48] was used to test whether $\mathbf{M}_s$ is positive semi-definite, but this was never found to be the case. The reason for this is that while $\mathbf{M}_s$ is always symmetrical, at least one of its first few eigenvalues is negative. However, because the ratio of the magnitude of these negative eigenvalues to the largest eigenvalue is always less than ϵ, to numerical precision $\mathbf{M}_s$ is positive semi-definite, therefore the technique complies with the covariance transport equation to the accuracy ϵ.

Because the timestep was relatively small compared to τ_c, the maximum error in **L** when applying no iterations was found to be approximately $\epsilon_{c,j} = 10^{-2}$, so this case is considered to be unconservative. Fig. 1 shows the centreline mixture fraction rms for $\tau_c/\tau = 1/8$ [16] for a range of error tolerances. Improving the conservation slightly increased the mixture fraction rms and consequently delayed the major heat release. However, the 95% confidence intervals for each variable and each error tolerance are sufficiently broad to overlap for each error tolerance, so all results are statistically identical: the technique does not significantly change MMC-IEM.

The error in conservation for **L** (Table 1) closely matches ϵ for sufficiently-small values of ϵ. Because almost every instance of **L** in the current simulations has an error less than 10^{-2}, decreasing ϵ causes an increasing fraction of locations to apply the technique of Section 4. While this is the nominal input error, the output error is measured by the absolute error in the mean mixture fraction caused by the mixing defined by **L**. For the homogeneous case [47], this error was 5 orders of magnitude lower than ϵ, whereas here this error is 3 orders of magnitude lower (Table 1). This demonstrates that the nominal error tolerance ϵ is more powerful and a certain precision in the results can be achieved with a more relaxed tolerance, saving computational effort.

Table 1 also shows the relative increase in the mean computational time required for each error level. Because very few instances of **L** had errors greater than 10^{-2}, there is unsurprisingly only an inconsequential increase in computational time to apply $\epsilon = 10^{-3}$. The computational time appears to grow exponentially with each decade that ϵ is reduced, but the error in **L** also asymptotically approaches ϵ within this data set (indicating that almost every instance of **L** has an error greater than $\epsilon = 10^{-5}$), so it is expected that each further reduction in ϵ by a decade would increase computational effort by approximately 2% in the current simulations.

The remaining results are all for $\epsilon = 10^{-5}$ and for reference previous BLM-MMC-Curl results using the same code and chemical kinetics [21] are also shown. The prediction of the centreline mean mixture fraction value (Fig. 2) is consistent irrespective of the parametric choices. The standard value [16] for the timescale ratio $\tau_c/\tau = 1/8$ predicts satisfactorily the mixture fraction rms (Fig. 3) upstream of the major heat release ($z/d < 40$), but under-predicts the experiment for essentially

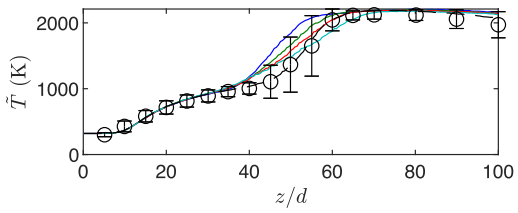

Fig. 4. Ensemble mean of centreline Favre-averaged temperature. As per Fig. 2.

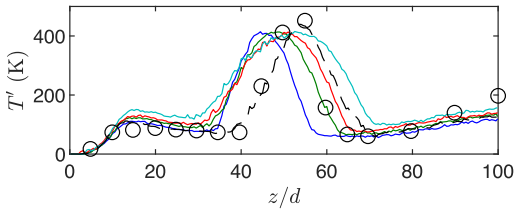

Fig. 5. Ensemble mean of centreline Favre-averaged temperature rms. As per Fig. 2.

the rest of the domain. Increasing τ_c/τ reduces the intensity of mixing, resulting in progressively-increased values of the rms. It is likely that τ_c/τ needs to be varied according to the turbulent intensity, consistent with previous findings for a homogeneous combustion case [17], where it was found that an increased τ_c/τ was required for a passive scalar case.

This variation in mixture fraction rms governs the location of the flame's front and its thickness: the mean temperature (Fig. 4) shows that the flame advances slightly as τ_c/τ increases, while the flame is also substantially broadened. This is because increasing τ_c/τ increases the conditional fluctuations [17], which reduces the likelihood of fuel and oxidiser particles interacting, thereby increasing the mixing duration. The parameter τ_c/τ has long been recognised as critical for modelling MMC in particular [16] because it can tune the model to a desired flame width; this parameter is also inherent in any turbulent combustion model, even if it is not explicitly determined or parameterised. All of the cases commence the major heat release significantly before the experiment, with $\tau_c/\tau = 1/8$ providing the closest match to the flame thickness, but higher values more closely matching the experiment through the major heat release zone because the flame for $\tau_c/\tau = 1/8$ finishes sooner. This behaviour is replicated in the temperature rms (Fig. 5) and species (Fig. 6).

The mixture fraction probability density function (pdf) (Fig. 7) demonstrates broad agreement with the experiment, with increasing values of τ_c/τ delaying the mixing of the coflow and fuel stream. The effect of the parameters can be clearly seen in the scatter plots of temperature as a function of mixture fraction (Fig. 8). Increasing τ_c/τ permits greater conditional fluctuations, which causes more of the lean particles to be able to approach chemical equilibrium early on. This, however, delays the major heat release $40 \leq z/d \leq 60$ from the rich particles because of the reduced rate of mixing of the unmixed fuel and coflow with the burning particles. It is this reduced rate of mixing that advances the flame compared to the experiment and BLM-MMC-Curl because there is insufficient local extinction in the vicinity of $z/d = 40$.

6. Conclusions

A technique to impose conservation – to numerical precision – on a mixing model that is not inherently conservative is shown to satisfy all mathematical criteria for a mixing process without significantly altering the mixing process. The MMC-IEM model is identified as being a model that is not conservative if the stochastic particles are assigned different weights (probabilities), which is a common procedure in inhomogeneous solvers. The technique is tested using the BLM-MMC

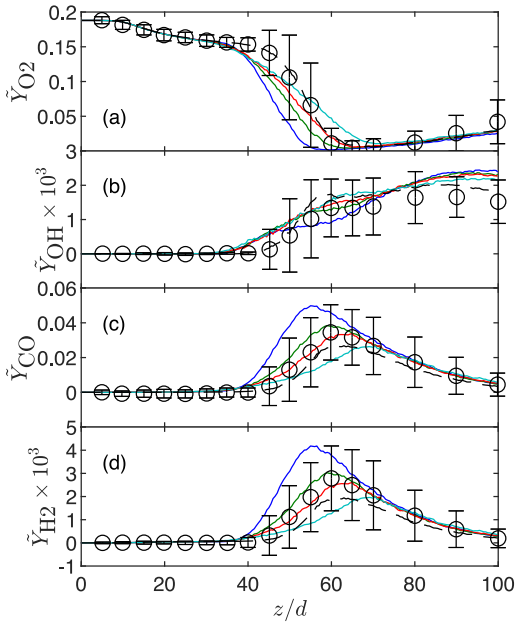

Fig. 6. Ensemble mean of centreline Favre-averaged mass fractions. (a) O_2; (b) OH; (c) CO; (d) H_2. Lines as per Fig. 2.

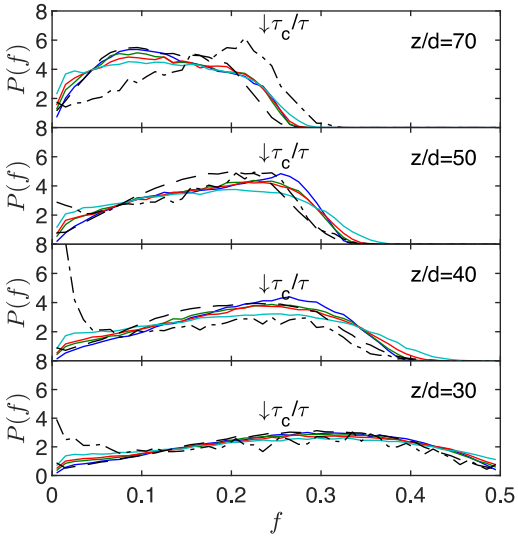

Fig. 7. Mixture fraction pdf at different axial locations. BLM-MMC as per Fig. 2; Experiment [35]: – ·.

framework for a jet that produces a lifted flame containing significant extinction-reignition. The model provides satisfactory agreement with the experiment, although it is noted that the timescale ratio τ_c/τ may need to vary to respond to the local turbulent conditions, consistent with previous findings for homogeneous combustion [17].

In the current work, a single reference variable was considered. While the technique to make the model conservative can be applied to MMC-IEM with multiple reference variables, there are additional complications that need to be resolved in multi-dimensional space. This is because in a single dimension each particle influences the mixing of precisely two particles; in multiple dimensions, each particle can influence the mixing of any number of particles – including zero. Future work will determine how to specify MMC-IEM so that the conservation technique is effective for multiple reference variables and also apply this technique to the PSP model.

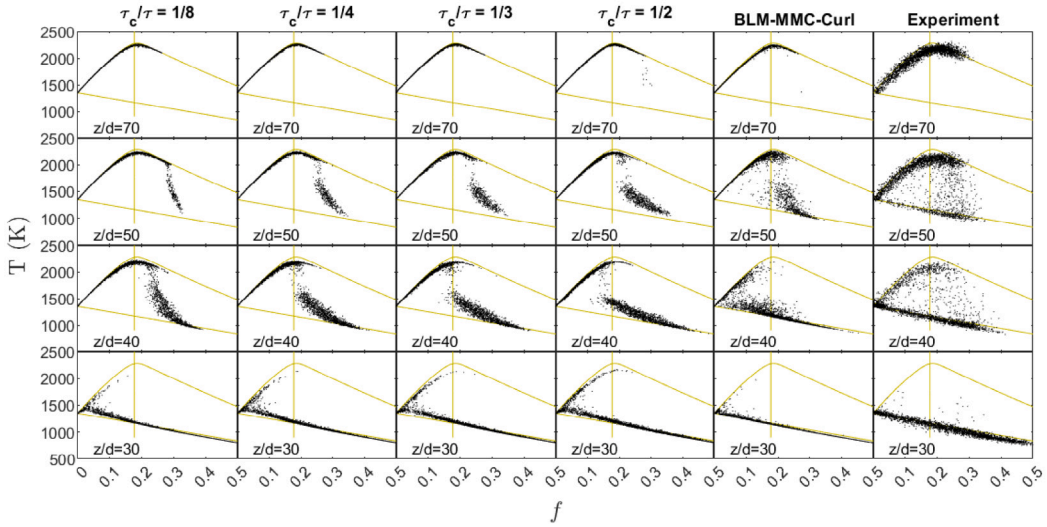

Fig. 8. Scatter plots of temperature, varying with mixture fraction. The right column is the experiment [35], the column beside that is BLM-MMC-Curl [21]. The vertical yellow lines indicate the stoichiometric mixture fraction, while the yellow upper curve indicates chemical equilibrium and the yellow lower angled line represents frozen conditions. (For interpretation of the references to colour in this figure legend, the reader is referred to the web version of this article.)

Novelty and significance statement

The novelty of this research is a new technique to make mixing models conservative within an error tolerance, applied to the MMC-IEM model which is not conservative for inhomogeneous simulations that use varying particle weights. It is significant because it permits MMC-IEM with a single reference variable (and other micro-mixing models) to be used without concerns that a lack of conservation in the formulation will create unphysical behaviour in the chemistry solver.

Declaration of competing interest

The authors declare that they have no known competing financial interests or personal relationships that could have appeared to influence the work reported in this paper.

Acknowledgements

The author is grateful to Prof. A.Y. Klimenko for inspiration in devising this technique, Prof. E.R. Hawkes for discussions that led to this application, and Prof. R.P. Lindstedt for the use of the PIPER code to conduct the simulations. This research was undertaken using the University of Southern Queensland (UniSQ) Fawkes HPC.

Appendix. Proof that MMC-IEM is only conservative if all weights are equal

To determine if Eq. (14) is conservative, consider:

$$\begin{aligned}\sum_i M_{ij} &= \sum_i \frac{W_i}{\tau_c}\left\{\delta_{ij} - \left[\frac{W_{j+1}}{W_{j-1}+W_{j+1}}\delta_{i(j+1)} + \frac{W_{j-1}}{W_{j-1}+W_{j+1}}\delta_{i(j-1)}\right]\right\}\\ &= \frac{1}{\tau_c}\left[W_j - \left(\frac{W_j^2}{W_{j-2}+W_j} + \frac{W_j^2}{W_j+W_{j+2}}\right)\right]\\ &= \frac{W_j}{\tau_c}\left[1 - W_j\frac{(W_j+W_{j+2})+(W_{j-2}+W_j)}{(W_{j-2}+W_j)(W_j+W_{j+2})}\right]\\ &= \frac{W_j}{\tau_c}\left[1 - \frac{W_j(W_{j-2}+W_j+W_{j+2})+W_j^2}{W_j(W_{j-2}+W_j+W_{j+2})+W_{j-2}W_{j+2}}\right].\end{aligned}$$

To satisfy Eq. (5) requires

$$W_j^2 = W_{j-2}W_{j+2}\,; \tag{23}$$

this is only generally possible if $\forall_j W_j = W$, i.e. all particles have identical weights.

References

[1] V. Viswanathan, A.H. Epstein, Y.-M. Chiang, E. Takeuchi, M. Bradley, J. Langford, M. Winter, The challenges and opportunities of battery-powered flight, Nature 601 (2022) 519–525.
[2] D.J. Beerer, V.G. McDonell, Autoignition of hydrogen and air inside a continuous flow reactor with application to lean premixed combustion, J. Eng. Gas Turbines Power 130 (2008) 051507–051514.
[3] S. Li, W. Qian, H. Liu, G. Liu, M. Zhu, Autoignition and flame lift-off behavior of a fuel jet mixing with turbulent hot air coflow, Proc. Combust. Inst. 38 (4) (2021) 6385–6392.
[4] A. Giusti, E. Mastorakos, Turbulent combustion modelling and experiments: Recent trends and developments, Flow, Turb. Combust. 103 (2019) 849–869.
[5] A.Y. Klimenko, S.B. Pope, A model for turbulent reactive flows based on multiple mapping conditioning, Phys. Fluids 15 (7) (2003) 1907–1925.
[6] S.K. Ghai, S. De, K. Vogiatzaki, M.J. Cleary, Theory and application of multiple mapping conditioning for turbulent reactive flows, in: S. De, A.K. Agarwal, S. Chaudhuri, S. Sen (Eds.), Modeling and Simulation of Turbulent Combustion, Energy, Environment, and Sustainability, Springer, Singapore, 2018, pp. 447–474.
[7] S. Subramaniam, S.B. Pope, A mixing model for turbulent reactive flows based on Euclidean minimum spanning trees, Combust. Flame 115 (4) (1998) 487–514.
[8] K. Luo, H. Pitsch, M. Pai, O. Desjardins, Direct numerical simulations and analysis of three-dimensional *n*-heptane spray flames in a model swirl combustor, Proc. Combust. Inst. 33 (2) (2011) 2143–2152.
[9] J. Villermaux, J.-C. Devillon, Representation of the coalescence and the redispersion of the fields of segregation in a fluid by a model of phenomenologic interaction, in: Chemical Reaction Engineering: Proceedings of the Fifth European/Second International Symposium on Chemical Reaction Engineering, Elsevier, Publishing Company, Amsterdam, Netherlands, 1972, pp. B1–13–B1–24.
[10] C. Dopazo, E.E. O'Brien, An approach to the autoignition of a turbulent mixture, Acta Astronaut. 1 (1974) 1239–1266.
[11] S.B. Pope, Lagrangian PDF methods for turbulent flows, Annu. Rev. Fluid Mech. 26 (1994) 23–63.
[12] R.O. Fox, On velocity–conditioned scalar mixing in homogeneous turbulence, Phys. Fluids 8 (10) (1996) 2678–2691.
[13] S.B. Pope, The vanishing effect of molecular diffusivity on turbulent dispersion: implications for turbulent mixing and the scalar flux, J. Fluid Mech. 359 (1998) 299–312.
[14] C. Dopazo, Relaxation of initial probability density functions in the turbulent convection of scalar fields, Phys. Fluids 22 (1979) 20–30.
[15] J. Janicka, W. Kolbe, W. Kollmann, Closure of the transport equation for the probability density function of turbulent scalar fields, J. Non-Equilib. Thermodyn. 4 (1) (1979) 47–66.
[16] A.P. Wandel, A.Y. Klimenko, Testing multiple mapping conditioning mixing for Monte Carlo probability density function simulations, Phys. Fluids 17 (12) (2005) 128105.
[17] A.P. Wandel, Conditional dissipation of scalars in homogeneous turbulence: Closure for MMC modelling, Combust. Theory Model. 17 (4) (2013) 707–748.
[18] A.P. Wandel, R.P. Lindstedt, Hybrid binomial Langevin–MMC modeling of a reacting mixing layer, Phys. Fluids 21 (1) (2009) 015103.

[19] A.P. Wandel, R.P. Lindstedt, Hybrid multiple mapping conditioning modeling of local extinction, Proc. Combust. Inst. 34 (2013) 1365–1372.
[20] A.P. Wandel, R.P. Lindstedt, A mixture-fraction-based hybrid binomial Langevin-multiple mapping conditioning model, Proc. Combust. Inst. 37 (2019) 2151–2158.
[21] M. du Preez, A.P. Wandel, D. Bontch-Osmolovskaia, R.P. Lindstedt, Parametric sensitivities of the generalised binomial Langevin–multiple mapping conditioning model, Phys. Fluids 33 (4) (2021) 045109.
[22] M.J. Cleary, A.Y. Klimenko, J. Janicka, M. Pfitzner, A sparse-Lagrangian multiple mapping conditioning model for turbulent diffusion flames, Proc. Combust. Inst. 32 (2009) 1499–1507.
[23] M.J. Cleary, A.Y. Klimenko, A generalised multiple mapping conditioning approach for turbulent combustion, Flow, Turb. Combust. 82 (2009) 477–491.
[24] C. Straub, S. De, A. Kronenburg, K. Vogiatzaki, The effect of timescale variation in multiple mapping conditioning mixing of PDF calculations for Sandia Flame series D—F, Combust. Theory Model. 20 (5) (2016) 894–912.
[25] S.K. Ghai, S. De, A. Kronenburg, Numerical simulations of turbulent lifted jet diffusion flames in a vitiated coflow using the stochastic multiple mapping conditioning approach, Proc. Combust. Inst. 37 (2019) 2199–2206.
[26] S.K. Ghai, S. De, Numerical investigation of auto-igniting turbulent lifted CH_4/air jet diffusion flames in a vitiated co-flow using a RANS based stochastic multiple mapping conditioning approach, Combust. Flame 203 (2019) 362–374.
[27] A. Varna, M.J. Cleary, E.R. Hawkes, A multiple mapping conditioning mixing model with a mixture-fraction like reference variable. Part 1: Model derivation and ideal flow test cases, Combust. Flame 181 (2017) 342–353.
[28] A. Varna, M.J. Cleary, E.R. Hawkes, A multiple mapping conditioning mixing model with a mixture-fraction like reference variable. Part 2: RANS implementation and validation against a turbulent jet flame, Combust. Flame 181 (2017) 354–364.
[29] C. Yu, P. Breda, M. Pfitzner, U. Maas, The hierarchy of low-dimensional manifolds in the context of multiple mapping conditioning mixing model, Proc. Combust. Inst. 39 (2023) 2299–2308.
[30] Z. Li, E.R. Hawkes, A. Wehrfritz, B. Savard, A DNS evaluation of three MMC-like mixing models for transported PDF modelling of turbulent nonpremixed flames, Combust. Flame 258 (2023) 113039.
[31] D.W. Meyer, P. Jenny, A mixing model for turbulent flows based on parameterized scalar profiles, Phys. Fluids 18 (2006) 035105.
[32] A.P. Wandel, Development of Multiple Mapping Conditioning (MMC) for Application to Turbulent Combustion (Ph.D. thesis), Division of Mechanical Engineering, The University of Queensland, 2005.
[33] T. Hůlek, R.P. Lindstedt, Joint scalar-velocity pdf modelling of finite rate chemistry in a scalar mixing layer, Combust. Sci. Tech. 136 (1998) 303–331.
[34] L. Valiño, C. Dopazo, A binomial Langevin model for turbulent mixing, Phys. Fluids A 3 (12) (1991) 3034–3037.
[35] R. Cabra, J.-Y. Chen, R.W. Dibble, A.N. Karpetis, R.S. Barlow, Lifted methane—air jet flames in a vitiated coflow, Combust. Flame 143 (2005) 491–506.
[36] P. Domingo, L. Vervisch, D. Veynante, Large-eddy simulation of a lifted methane jet flame in a vitiated coflow, Combust. Flame 152 (2008) 415–432.
[37] M. Ihme, Y.C. See, Prediction of autoignition in a lifted methane/air flame using an unsteady flamelet/progress variable model, Combust. Flame 157 (2010) 1850–1862.
[38] O. Schulz, T. Jaravel, T. Poinsot, B. Cuenot, N. Noiray, A criterion to distinguish autoignition and propagation applied to a lifted methane–air jet flame, Proc. Combust. Inst. 36 (2017) 1637–1644.
[39] P. Simatos, L. Tian, R. Lindstedt, The impact of molecular diffusion on auto-ignition in a turbulent flow, Combust. Flame 239 (2022) 111665.
[40] M.R. Malik, A. Coussement, T. Echekki, A. Parente, Principal component analysis based combustion model in the context of a lifted methane/air flame: Sensitivity to the manifold parameters and subgrid closure, Combust. Flame 244 (2022) 112134.
[41] R. Amaduzzi, A. Bertolino, A. Özden, R. Malpica Galassi, A. Parente, Impact of scalar mixing uncertainty on the predictions of reactor-based closures: Application to a lifted methane/air jet flame, Proc. Combust. Inst. 39 (4) (2023) 5165–5175.
[42] R.P. Lindstedt, S. Louloudi, E. Váos, Joint scalar probability density function modelling of pollutant formation in piloted turbulent jet diffusion flames with comprehensive chemistry, Proc. Combust. Inst. 28 (2000) 149–156.
[43] R. Lindstedt, S. Louloudi, J. Driscoll, V. Sick, Finite rate chemistry effects in turbulent reacting flows, Flow, Turb. Combust. 72 (2004) 407–426.
[44] C.G. Speziale, S. Sarkar, T.B. Gatski, Modelling the pressure–strain correlation of turbulence: an invariant dynamical systems approach, J. Fluid Mech. 227 (1991) 245–272.
[45] B.J. Daly, F.H. Harlow, Transport equations in turbulence, Phys. Fluids 13 (1970) 2634–2649.
[46] W.P. Jones, Turbulence modelling and numerical solution methods for variable density and combusting flows, in: P.A. Libby, F.A. Williams (Eds.), Turbulent Reacting Flows, Academic Press, New York, 1993, pp. 309–374.
[47] A.P. Wandel, MMC-IEM with varying particle weights: A numerically-conservative method for a single reference variable, in: Proceedings of the 2023 Australian Combustion Symposium, 2023.
[48] Note sur une méthode de résolution des équations normales provenant de l'application de la méthode des moindres carrés à un système d'équations linéaires en nombre inférieur à celui des inconnues. — Application de la méthode a la résolution d'un système defini d'équations linéaires, Bull. Géodésique 2 (1) (1924) 67–77.